Published April 2, 2001

FtsZ Ring Formation at the Chloroplast Division Site in Plants

Stanislav Vitha, Rosemary S. McAndrew, and Katherine W. Osteryoung

Department of Plant Biology, Michigan State University, East Lansing, Michigan 48824

Abstract. Among the events that accompanied the evolution of chloroplasts from their endosymbiotic ancestors was the host cell recruitment of the prokaryotic cell division protein FtsZ to function in chloroplast division. FtsZ, a structural homologue of tubulin, mediates cell division in bacteria by assembling into a ring at the midcell division site. In higher plants, two nuclear-encoded forms of FtsZ, FtsZ1 and FtsZ2, play essential and functionally distinct roles in chloroplast division, but whether this involves ring formation at the division site has not been determined previously. Using immunofluorescence microscopy and expression of green fluorescent protein fusion proteins in *Arabidopsis thaliana*, we demonstrate here that FtsZ1 and FtsZ2 localize to coaligned rings at the chloroplast midpoint. Antibodies specific for recognition of FtsZ1 or FtsZ2 proteins in *Arabidopsis* also recognize related polypeptides and detect midplastid rings in pea and tobacco, suggesting that midplastid ring formation by FtsZ1 and FtsZ2 is universal among flowering plants. Perturbation in the level of either protein in transgenic plants is accompanied by plastid division defects and assembly of FtsZ1 and FtsZ2 into filaments and filament networks not observed in wild-type, suggesting that previously described FtsZ-containing cytoskeletal-like networks in chloroplasts may be artifacts of *FtsZ* overexpression.

Key words: plastids • organelle replication • organelle fission • cytoskeleton • mitochondria

Introduction

Chloroplasts are the site of photosynthesis, the process which most organisms, including humans, rely on directly or indirectly for their source of organic compounds and energy. These double-membrane organelles arise by differentiation from their undifferentiated precursors, proplastids, which are present primarily in the mitotic cells of the meristem. There, proplastids must divide to maintain their numbers in new daughter cells. As plant cells mature, they enlarge and differentiate, and during this process the chloroplasts in the mesophyll cells of the leaf undergo several additional rounds of replication. In *Arabidopsis thaliana*, leaf mesophyll cells ultimately contain over 100 chloroplasts, compared with 14 proplastids in meristematic cells (Pyke and Leech, 1992). Thus, proplastid and chloroplast division are essential both for maintaining plastid populations in dividing cells and for achieving maximum photosynthetic capacity in mature leaves (Leech, 1976; Leech and Baker, 1983).

In recent years, it has been discovered that the division of chloroplasts, which evolved from a cyanobacterial endosymbiont (Martin et al., 1998; Gray, 1999; McFadden, 1999), shares similarities with bacterial cytokinesis. Both chloroplasts and bacteria divide by binary fission, in which a division furrow forms at the midpoint and then constricts until the two daughter cells or chloroplasts separate. Although division of bacteria requires cell wall peptidoglycan synthesis at the division septum as well as constriction of the cytoplasmic membrane, division of chloroplasts, which lack the peptidoglycan wall, requires the constriction and severing of two envelope membranes. A key player in the division of both bacteria and chloroplasts is FtsZ, a prokaryotic cytoskeletal GTPase that self-assembles in vitro into filaments and other conformations similar to those formed by its eukaryotic structural homologue, tubulin (Bi and Lutkenhaus, 1991; Erickson et al., 1996; Bramhill, 1997; Lutkenhaus and Addinall, 1997; Löwe and Amos, 1998; Rothfield et al., 1999; Margolin, 2000). In bacteria, FtsZ functions in cell division by assembling into a contractile ring at the midcell division site. The formation of the FtsZ ring is the first known step in division and is essential for the recruitment of all other bacterial cell division proteins to the division site to form a functional division apparatus. Precise positioning of the FtsZ ring to the cell center in *Escherichia coli* is dictated in part by the activity of MinD, which acts in concert with two other proteins to prevent FtsZ ring assembly at inappropriate sites (de Boer et al., 1989; Raskin and de Boer, 1997, 1999a,b). It has been shown recently that nuclear-encoded forms of FtsZ and MinD also mediate the division of plastids in plants (Osteryoung et al., 1998; Strepp et al., 1998; Colletti et al., 2000; Kanamaru et al., 2000), indicating that bacterial cell and chloroplast division are evolutionarily and mech-

The online version of this article contains supplemental material.

Address correspondence to Katherine Osteryoung, Department of Plant Biology, 166 Plant Biology Building, Michigan State University, East Lansing, MI 48824. Tel.: (517) 355-4685. Fax: (517) 353-1926. E-mail: osteryou@msu.edu

Supplemental Material can be found at:
/content/suppl/2001/03/30/153.1.111.DC1.html

Published April 2, 2001

anistically related. FtsZ genes are also present in the prokaryotic relatives of mitochondria and presumably participate in mitochondrial division in algae and other protists (Beech and Gilson, 2000; Beech et al., 2000; Takahara et al., 2000), but are not found in fungi or animals where their functions in organelle division have apparently been taken over by another type of self-assembling GTPase, dynamin (Erickson, 2000; Osteryoung, 2000).

The majority of bacterial species studied thus far possess a single *ftsZ* gene. However, *A. thaliana* and other vascular plants carry at least two nuclear-encoded FtsZ homologues that each fall into one of two structurally and functionally distinct protein families, FtsZ1 and FtsZ2 (Osteryoung et al., 1998; Osteryoung and McAndrew, 2001). All members of the FtsZ1 family identified thus far are predicted to bear cleavable chloroplast transit peptides, and FtsZ1 gene products from *Arabidopsis* and pea have been shown experimentally to be imported into isolated chloroplasts in vitro (Osteryoung and Vierling, 1995; Gaikwad et al., 2000). In contrast, many members of the FtsZ2 family are not predicted to contain chloroplast transit peptides (Osteryoung and McAndrew, 2001). Despite the difference in predicted localization, *AtFtsZ1-1* and *AtFtsZ2-1*, *Arabidopsis* members of the *FtsZ1* and *FtsZ2* gene families, respectively, have both been shown by antisense repression to play essential, nonredundant roles in chloroplast division (Osteryoung et al., 1998). To integrate these findings with those from ultrastructural studies revealing concentric, electron-dense "plastid-dividing (PD)[1] rings" positioned on the stromal and cytosolic surfaces of the envelope membranes in the constricted neck of dividing chloroplasts (Kuroiwa et al., 1998), a working model was proposed in which FtsZ1 and FtsZ2 were hypothesized to cooperate in chloroplast constriction as components of the stromal and cytosolic PD rings, respectively. However, FtsZ1-like proteins have not been identified in nonvascular plants and two functionally distinct FtsZ2-like proteins from the moss *Physcomitrella patens*, which are essential for chloroplast division in that organism, are both localized in the stromal compartment of the chloroplast (Strepp et al., 1998; Kiessling et al., 2000). Thus, the relationship between predicted localization and function in plastid division remains uncertain. In addition, recent descriptions of a third PD ring localized in the intermembrane space (Miyagishima et al., 1998) have raised the possibility that plant FtsZ proteins could reside in this chloroplast subcompartment as well.

A key prediction of the model described above, irrespective of the suborganellar localizations of FtsZ1 and FtsZ2, is that both proteins function in plastid division via ring formation at the division site. To begin testing this model, we investigated the localization of FtsZ1 and FtsZ2 by immunofluorescence microscopy. In addition, we generated transgenic *Arabidopsis* plants producing a green fluorescent protein (GFP)-tagged form of AtFtsZ1-1, allowing us to visualize the fusion protein in living plant cells. Here, we show for the first time that FtsZ1 and FtsZ2 proteins both localize to rings at the plastid midpoint. We further demonstrate that increased or decreased levels of these proteins are accompanied by the formation of FtsZ-containing filament networks and concomitant defects in plastid division.

[1]*Abbreviations used in this paper:* GFP, green fluorescent protein; CaMV, cauliflower mosaic virus; PD, plastid-dividing.

Materials and Methods

Plant Material

Wild-type *A. thaliana*, ecotype Columbia (Col-0), transgenic plants expressing *AtFtsZ1-1* or *AtFtsZ2-1* antisense transgenes (Osteryoung et al., 1998), the *Arabidopsis* chloroplast division mutant *arc5* (Landsberg *erecta* background) (Robertson et al., 1996), and tobacco (*Nicotiana tabacum*) cv. 'Petit Havana' were grown for 4 wk in a growth chamber as described previously (Osteryoung et al., 1998). Pea (*Pisum sativum*) cv. 'Little Marvel' seeds were germinated in vermiculite and grown for 10 d under the same conditions.

Construction of AtFtsZ1-1–GFP Transgene

A fragment from the *AtFtsZ1-1* genomic sequence was amplified by PCR from *Arabidopsis* bacterial artificial chromosome clone MCO15 (EMBL/GenBank/DDBJ accession number AB010071), using primers 5′-GAAGGATCCCAGACACTTTCTC (forward) and 5′-AACTGGATCCAAAGTCTACGGGG (reverse) designed to create a BamHI restriction site (underlined). The ~3.5-kb amplification product, after digestion with BamHI, contained ~1.67 kb of the 5′ region and the entire coding sequence of *AtFtsZ1-1*, excluding the ultimate phenylalanine and stop codons. This fragment was inserted into the BamHI site in front of a soluble-modified GFP (EMBL/GenBank/DDBJ accession number U70495) (Davis and Vierstra, 1996) cassette, psmGFP (stock number CD3-326; *Arabidopsis* Biological Resource Center) containing GFP and a *nos* terminator, in the pBJ97 shuttle vector (empty vector obtained from Bart Janssen, The Horticulture and Food Research Institute, Auckland, New Zealand via John Bowman, University of California at Davis, Davis, CA). Sequencing confirmed that no PCR amplification errors were introduced into the coding sequence of *AtFtsZ1-1* and that the *AtFtsZ1-1* insert was in frame with the GFP coding sequence. In the resulting fusion protein, the penultimate phenylalanine of AtFtsZ1-1 was changed to tryptophan (underlined) and a linker region before the starting methionine of GFP encoded the sequence WIGGSIQGDIT. The *AtFtsZ1-1*–GFP construct was then excised with NotI and inserted into the plant transformation vector pMLBART (obtained from Karl Gordon, Commonwealth Scientific and Industrial Research Organization, Canberra, Australia via John Bowman, University of California at Davis, Davis, CA), a derivative of pART27 (Gleave, 1992), that confers resistance to the herbicide glufosinate as a selectable marker.

Plant Transformation and Growth

Agrobacterium-mediated transformation of *Arabidopsis* wild-type and *arc5* mutant plants and growth of the T_1 generation of transgenics were performed as described (Osteryoung et al., 1998). T_1 seedlings were sprayed three times at 7, 11, and 15 d with Finale (Agrevo) herbicide containing 120 mg/liter glufosinate ammonium as the active compound and 250 μl/liter Silwett L-77 (OSi Specialties, Inc.) added as a detergent. Leaves from the surviving plants were screened under a microscope for chloroplast phenotypes and GFP fluorescence. Plants were grown to maturity and T_2 seeds were collected. For analysis of the T_2 generation, plants were sown on Rockwool (GrodanHP; Agro Dynamics) saturated with a Hoagland's nutrient solution and grown for 4 wk under the same conditions as the T_1 plants. The first three leaves were harvested for immunoblot analysis and the fourth leaf was used for microscopy. Chloroplast numbers in mesophyll cells from these leaves were determined as described previously (Osteryoung et al., 1998).

Antibodies

Antipeptide antibodies against AtFtsZ1-1 and AtFtsZ2-1 were raised in rabbits and affinity-purified as described (Stokes et al., 2000). The final protein concentration was 0.3 and 0.9 mg/ml for the anti–AtFtsZ1-1 and anti–AtFtsZ2-1 antibodies, respectively.

Immunofluorescence

Tissue from the base of expanding, young 15-mm-long leaves was fixed in FAA (3% formaldehyde, 5% acetic acid, 50% ethanol) at room temperature overnight and embedded in low-melting polyester wax (Steedman's wax; Steedman, 1957) at 37°C as described (Vitha et al., 2000). 7-μm-thick

Published April 2, 2001

paradermal sections were attached to poly-L-lysine–coated glass slides, dewaxed, and rehydrated (Vitha et al., 2000). The sections were then subjected to an antigen retrieval procedure (Shi et al., 1997) by submerging the slides in 0.1 M Tris-HCl, pH 10.5, and autoclaving them in plastic Coplin jars for 10 min. Jars were then allowed to cool at room temperature for 30 min. Slides were transferred to blocking buffer (2% nonfat dry milk and 0.05% Tween 20 in PBS) for 30 min, then incubated for 3 h at room temperature with affinity-purified anti–AtFtsZ1-1 or anti–AtFtsZ2-1 antibodies at dilutions of 1:300 and 1:200, respectively, in incubation buffer (2% normal goat serum in blocking buffer). Slides were subsequently washed in blocking buffer (three times for 10 min), then incubated for 2 h with an FITC-conjugated anti–rabbit secondary antibody (Sigma-Aldrich) used at a dilution of 1:150. Control slides were treated similarly, except that preimmune serum was used instead as the primary antibody.

Double Immunofluorescence Labeling

Because both of the anti-AtFtsZ antibodies were raised in rabbit, a sequential labeling protocol was employed for double labeling (Negoescu et al., 1994). Antigen retrieval, antibody dilutions, and washing were the same as in the single immunofluorescence protocol above. Sections were incubated for 2 h with the first anti-AtFtsZ antibody and then with a monovalent anti–rabbit Rhodamine red–X conjugate (Jackson ImmunoResearch Laboratories) for 1.5 h at a dilution of 1:50. Any epitopes remaining exposed on the first anti-AtFtsZ antibody were blocked with unlabeled monovalent anti–rabbit antibody at a dilution of 1:50. Afterwards, slides were incubated for 2 h with the second anti-AtFtsZ antibody, followed by 2 h with a goat anti–rabbit FITC conjugate (Sigma-Aldrich) at a dilution of 1:50. Control sections were treated in a similar manner, except that either the second or both anti-AtFtsZ antibodies were omitted from the incubation mixture. Additionally, the sequence of application of the anti-AtFtsZ antibodies was reversed on some slides in order to compare the relative intensities of the fluorescence signals and determine whether elution of antibodies had occurred.

Microscopy

All samples were viewed using a microscope (BH2; Olympus) with a 100× 1.25 NA objective (Olympus). Bright-field images were obtained using differential interference contrast (Nomarski) optics. For epifluorescence, an FITC (excitation 455–495 nm, emission 512–575 nm) or Texas red (excitation 535–585 nm, emission 607–682 nm) filter set was used and images were recorded either on TMAX 400 film (Eastman Kodak Co.), or videocaptured with a color video camera (DEI 750; Optronics) and Scion Image v1.62 software (Scion Corporation). The z-series of optical sections were videocaptured using Scion Image software, with 0.5-μm steps between sections. All images were assembled for publication using Adobe Photoshop® 5.0 (Adobe Systems Inc.) and Canvas 6.0 (Deneba Software) software. For in vivo GFP fluorescence microscopy, fresh leaf tissue was mounted in water and viewed with an FITC filter set and images were recorded on TMAX 400 film (Eastman Kodak Co.).

Immunoblotting

Preparation of leaf extracts, PAGE, and immunoblotting were performed as described (Stokes et al., 2000). Extract from 1 mg fresh leaf tissue was loaded in each lane.

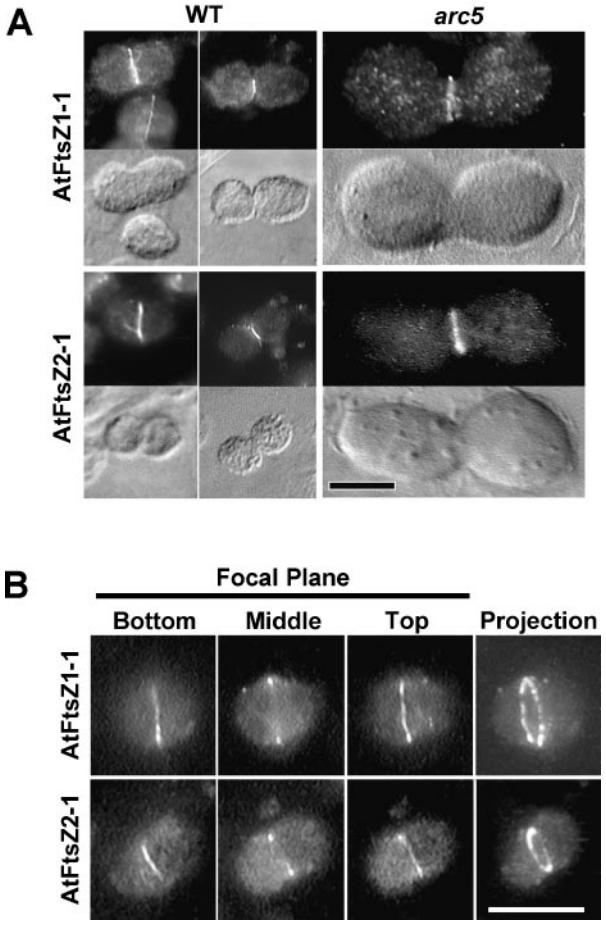

Figure 1. Immunofluorescence microscopy of AtFtsZ1-1 and AtFtsZ2-1 in *Arabidopsis*. Fixed, embedded leaf sections from 4-wk-old *Arabidopsis* plants were probed with affinity-purified polyclonal antibodies generated against peptides from either AtFtsZ1-1 or AtFtsZ2-1 (Stokes et al., 2000), followed by incubation with anti–rabbit secondary antibodies labeled with FITC. The fluorescence images in A, C, and D are accompanied by bright-field images to reveal the chloroplast shape. (A) Chloroplasts in sections from wild-type (left) and *arc5* (right) probed with anti–AtFtsZ1-1 (top) or anti–AtFtsZ2-1 (bottom). (B) Optical sections through the bottom, middle, or top of chloroplasts from wild-type sections labeled with anti–AtFtsZ1-1 (top) or anti–AtFtsZ2-1 (bottom). The stack of images was rotated 30% and projected to reveal the complete FtsZ ring (far right). (C) Labeled sections from wild-type plants showing that AtFtsZ1-1 (left) and AtFtsZ2-1 (right) rings are present in virtually all mesophyll cell chloroplasts. (D) AtFtsZ1-1 (left) and AtFtsZ2-1 (right) labeling in a chloroplast at a late stage of constriction. Arrows show filaments spiraling off the central ring. The three-dimensional projections of the stack of optical sections can be rotated in the two videos available at http://www.jcb.org/cgi/content/full/153/1/111/DC1. Bars, 5 μm.

Published April 2, 2001

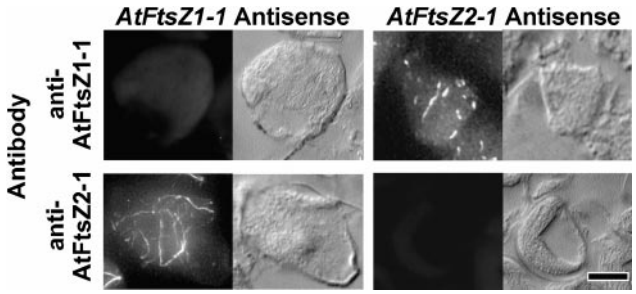

Figure 2. Specificity of anti–AtFtsZ1-1 and anti–AtFtsZ2-1 antibodies in situ. Leaf sections from *Arabidopsis* antisense plants depleted of either AtFtsZ1-1 (left) or AtFtsZ2-1 (right) (Stokes et al., 2000) were probed with affinity-purified antibodies directed against either AtFtsZ1-1 (top) or AtFtsZ2-1 (bottom). Labeling patterns were visualized by fluorescence microscopy. Chloroplast morphology is shown in adjacent bright-field images. Bar, 10 μm.

Online Supplemental Material

Fluorescence images in stacks of optical sections, captured as described above, were batch-processed using Adobe Photoshop® 5.0 (Filter-Despeckle, Filter-Unsharp Mask, Adjust Levels). Image stacks were then projected using Scion Image (Brightest Point Method, rotation angle increment 4°) and saved as a rotating projection into a video file. Videos containing animated versions of the data shown in Fig. 1 D can be viewed at http://www.jcb.org/cgi/content/full/153/1/111/DC1.

Results

AtFtsZ1-1 and AtFtsZ2-1 Localize to Rings at the Plastid Midpoint in Arabidopsis

Immunofluorescence microscopy was used to investigate the localization of FtsZ1 and FtsZ2 proteins in leaf sections from *Arabidopsis* both in wild-type plants and in the plastid division mutant *arc5*. The division site is easily visualized in *arc5* because the chloroplasts are arrested in division and remain permanently constricted (Robertson et al., 1996). Affinity-purified, antipeptide antibodies generated against AtFtsZ1-1 and AtFtsZ2-1, both with high specificity for their target proteins on immunoblots (Stokes et al., 2000), were employed for these studies. In both wild-type and *arc5*, anti–AtFtsZ1-1 and anti–AtFtsZ2-1 antibodies each detected immunoreactive proteins that localized to the chloroplast midpoint (Fig. 1 A). Three-dimensional reconstruction of images obtained from several focal planes revealed that both proteins were organized into clearly distinguishable, smoothly curved ring structures (Fig. 1 B). These rings appeared to be associated with the chloroplast periphery, though their precise positions relative to the chloroplast envelope membranes and to each other could not be determined. Localization of AtFtsZ1-1 and AtFtsZ2-1 to the plastid midpoint was evident in most mesophyll cell chloroplasts (Fig. 1 C) and in both constricted and nonconstricted chloroplasts, suggesting that the ring or rings remain assembled whether or not the chloroplasts are in the process of division. In deeply constricted chloroplasts, AtFtsZ1-1 and AtFtsZ2-1 were also frequently detected in one or more thin filaments emanating from the central ring (Fig. 1 D). Rotation of the three-dimensional image projections of optical sections through these structures revealed that the filaments spiraled along the chloroplast periphery (videos available at http://www.jcb.org/cgi/content/full/153/1/111/DC1) and suggested they could represent an intermediate stage in repositioning of the AtFtsZ1-1– and AtFtsZ2-1–containing rings to the center of the newly formed daughter plastids. Control sections in which the anti-AtFtsZ antibodies were either omitted or substituted with preimmune serum did not show significant staining (not shown).

To further confirm the in situ specificity of the anti–AtFtsZ1-1 and anti–AtFtsZ2-1 antibodies for their target proteins and to begin investigating the interdependence of AtFtsZ1-1 and AtFtsZ2-1 localization, immunofluorescence labeling was performed on transgenic *Arabidopsis* plants expressing *AtFtsZ1-1* or *AtFtsZ2-1* antisense transgenes that had been shown by immunoblotting to be depleted in the corresponding protein (Stokes et al., 2000). These plants are severely impaired in plastid division and contain single, large chloroplasts in their mesophyll cells (Osteryoung et al., 1998). The patterns of FtsZ localization in the two sets of antisense plants were distinct from one another and from those in wild-type. In the *AtFtsZ1-1* antisense plants, immunofluorescence labeling of AtFtsZ1-1 was not detected (Fig. 2, top left), but AtFtsZ2-1 could be detected in multiple filaments that did not show a specific pattern of localization (Fig. 2, bottom left). These filaments bent around the chloroplast periphery and in many cases were connected into rings and spirals encircling the enlarged chloroplasts, though these were often jagged rather than smoothly curved. In the *AtFtsZ2-1* antisense lines, AtFtsZ2-1 protein could not be detected by immunofluorescence staining (Fig. 2, bottom right), but AtFtsZ1-1 was detected largely in numerous short filaments and bright foci (Fig. 2, top right). Because these structures were too short to trace in three-dimensional reconstructions, it could not be determined reliably whether they were associated with the chloroplast periphery, the interior, or both. Some longer AtFtsZ1-1 filaments were also observed in these plants and generally appeared as single, discrete filaments, unlike the disorganized AtFtsZ2-1 filament networks seen in the *AtFtsZ1-1* antisense plants.

The data shown in Fig. 2 demonstrate that the antibody specificity observed on immunoblots (Stokes et al., 2000) is preserved during immunofluorescence staining and indicate that the rings and filaments detected by the anti–AtFtsZ1-1 and anti–AtFtsZ2-1 antibodies represent distinct proteins. We conclude that FtsZ1 and FtsZ2 both assemble into rings at the site of chloroplast constriction in *Arabidopsis*. In addition, the fact that AtFtsZ1-1–containing filaments were observed in the *AtFtsZ2-1* antisense plants and vice versa further suggests that FtsZ1 and FtsZ2 proteins are not dependent on one another for their assembly into cytoskeletal-like structures. The presence of FtsZ-containing rings in *arc5* (Fig. 1 A) indicates that the *ARC5* gene product acts after assembly of AtFtsZ1-1 and AtFtsZ2-1 into ring structures and suggests that FtsZ1 and FtsZ2 proteins are both involved in the initiation of plastid constriction.

AtFtsZ1-1 and AtFtsZ2-1 Rings Are Colocalized

To determine whether the AtFtsZ1-1 and AtFtsZ2-1 rings were colocalized, we performed sequential double-immunofluorescence labeling of leaf chloroplasts. This was necessary because both antibodies were raised in rabbits and therefore simultaneous double labeling was not feasible. When the digital images of the AtFtsZ1-1 and AtFtsZ2-1

Published April 2, 2001

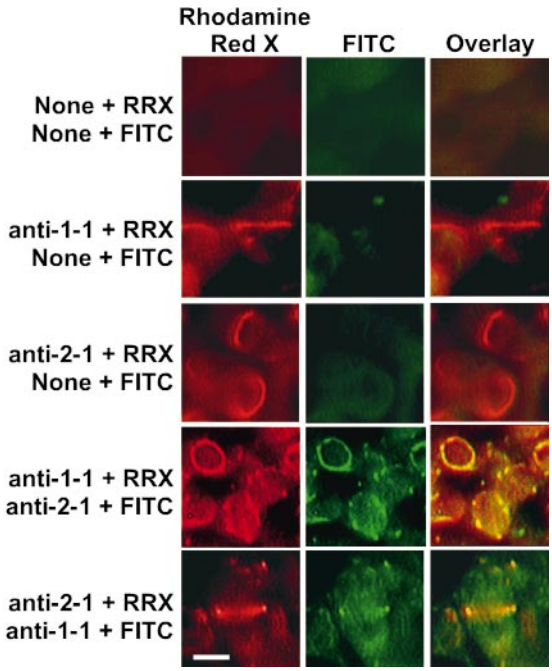

Figure 3. AtFtsZ1-1 and AtFtsZ2-1 rings are colocalized. Leaf sections from wild-type *Arabidopsis* plants were subjected to sequential, double immunofluorescence labeling of AtFtsZ1-1 and AtFtsZ2-1. The order of antibody application is indicated on the left. Tissue sections were incubated first with no antibodies (None), anti–AtFtsZ1-1 antibodies (anti–1-1), or anti–AtFtsZ2-1 antibodies (anti–2-1), followed by monovalent anti–rabbit antibody conjugated to Rhodamine red–X (RRX). Sections were then treated with no, anti–AtFtsZ1-1, or anti–AtFtsZ2-1 antibody, followed by anti–rabbit FITC conjugate. The labeled sections were viewed using FITC (green) and Texas red (red) filter sets. The yellow color in the overlay of the red and green signals indicates colocalization of AtFtsZ1-1 and AtFtsZ2-1. Bar, 2 μm.

localization patterns were superimposed, the fluorescence signals were precisely overlaid (Fig. 3, bottom two rows). A series of control treatments in which one or both antibodies were omitted demonstrated that immunodetection of each protein was specific in tissue sections and cross-talk between the AtFtsZ1-1 and AtFtsZ2-1 signals was minimal (Fig. 3, top three rows). The relative intensities of the two fluorescence signals were independent of the order of labeling, indicating that elution of antibodies during the labeling procedure was not significant (Fig. 3, compare last two rows). We conclude from these data that the AtFtsZ1-1– and AtFtsZ2-1–containing rings are coaligned.

GFP-tagged AtFtsZ1-1 Behaves Similarly to the Untagged Protein

As a prelude to studying chloroplast FtsZ localization dynamics in living tissue, we constructed a gene encoding AtFtsZ1-1 fused to GFP. A COOH-terminal GFP fusion was used since AtFtsZ1-1 contains an NH_2-terminal transit peptide that is processed upon import to the chloroplast (Osteryoung and Vierling, 1995). Because overexpression of *AtFtsZ1-1* driven by the strong cauliflower mosaic virus (CaMV) 35S promoter inhibits chloroplast division (Stokes et al., 2000), the *AtFtsZ1-1*–GFP transgene was expressed under control of a 1.6-kb stretch of the native *AtFtsZ1-1* promoter in an effort to prevent overaccumulation of the fusion protein. Transgenic plants were produced in both wild-type and *arc5* backgrounds and fusion protein localization was investigated by in vivo fluorescence microscopy.

Although *AtFtsZ1-1* RNA levels are generally quite low in wild-type plants (Osteryoung et al., 1998; Stokes, K.D., and K.W. Osteryoung, unpublished observations), immunoblotting demonstrated that independent transgenic lines exhibited a wide range of AtFtsZ1-1–GFP levels, some of them very high, despite use of the *AtFtsZ1-1* promoter. This suggests that additional regulatory elements outside the promoter fragment used in transgene construction may participate in regulating expression of endogenous *AtFtsZ1-1*. Most of the transgenic plants produced in the wild-type background also exhibited defects in chloroplast division, as indicated by the presence of reduced numbers of enlarged chloroplasts. In plants with relatively low levels of AtFtsZ1-1–GFP (Fig. 4 A, lane 3), the fusion protein could be clearly observed as a single ring localized in the constricted neck of the chloroplasts (Fig. 4 B, left) and in nonconstricted chloroplasts (Fig. 4 C, left). These plants exhibited reduced numbers (10–20 per cell) of larger-than-normal chloroplasts when compared with wild-type, but constricted chloroplasts were seen frequently. AtFtsZ1-1–GFP rings were also localized to a single ring in constricted chloroplasts in the *arc5* background (Fig. 4 B, right).

In plants with high levels of AtFtsZ1-1–GFP (Fig. 4 A, lane 5), the fusion protein was detected in mesophyll cell chloroplasts in the form of many filaments that appeared to be randomly organized (Fig. 4 C, center). These plants exhibited more severe defects in chloroplast division, with ~70% of the mesophyll cells containing only a single giant chloroplast. In general, the severity of the chloroplast division defect appeared to be correlated with the level of AtFtsZ1-1–GFP accumulation and with the presence of AtFtsZ1-1–GFP filament networks. A similar correlation between AtFtsZ1-1 accumulation and plastid division inhibition has been demonstrated previously in plants overexpressing an *AtFtsZ1-1* transgene under control of the CaMV 35S promoter (Stokes et al., 2000). Among these overexpression lines, immunofluorescence staining of sections from individuals with severe plastid division defects and high AtFtsZ1-1 levels (Fig. 4 A, lane 7) revealed that AtFtsZ1-1 is also detected in disorganized filament networks in these plants (Fig. 4 C, right). AtFtsZ1-1–GFP was often localized similarly in the *arc5* background (not shown), but the inhibition of chloroplast division was only evident at highest expression levels, probably because *arc5* has a reduced number of enlarged chloroplasts to begin with (Robertson et al., 1996).

Among the plants with high levels of AtFtsZ1-1–GFP, chloroplasts in epidermal cells were not as grossly enlarged as in mesophyll cells, though many contained networks of AtFtsZ1-1–GFP filaments (Fig. 4 D). In the pavement cells of the epidermis, AtFtsZ1-1-GFP–containing strands extended from these chloroplasts, spanning long distances across the cell (Fig. 4 D, top left). These strands were often visible in bright-field images as well (Fig. 4 D, bottom left). In the guard cells of stomata, individual chloroplasts often seemed to be interconnected by the AtFtsZ1-1–GFP strands (Fig. 4 D, top right). These observation indicate that AtFtsZ1-1–GFP accumulates in thin connections between the chloroplast, which probably represent "stromules" described previously by Kohler et al. (1997).

Published April 2, 2001

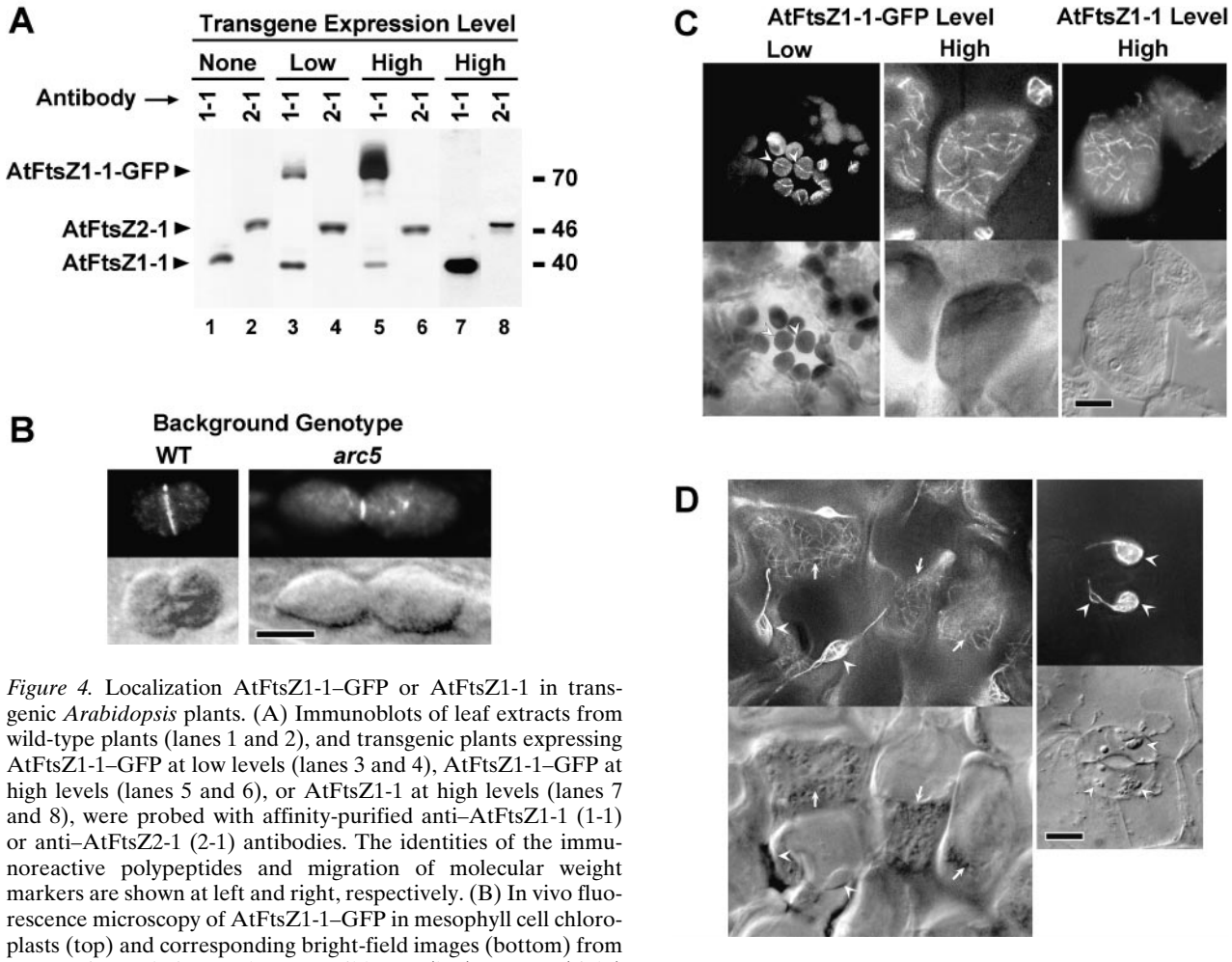

Figure 4. Localization AtFtsZ1-1–GFP or AtFtsZ1-1 in transgenic *Arabidopsis* plants. (A) Immunoblots of leaf extracts from wild-type plants (lanes 1 and 2), and transgenic plants expressing AtFtsZ1-1–GFP at low levels (lanes 3 and 4), AtFtsZ1-1–GFP at high levels (lanes 5 and 6), or AtFtsZ1-1 at high levels (lanes 7 and 8), were probed with affinity-purified anti–AtFtsZ1-1 (1-1) or anti–AtFtsZ2-1 (2-1) antibodies. The identities of the immunoreactive polypeptides and migration of molecular weight markers are shown at left and right, respectively. (B) In vivo fluorescence microscopy of AtFtsZ1-1–GFP in mesophyll cell chloroplasts (top) and corresponding bright-field images (bottom) from transgenic *Arabidopsis* plants of wild-type (left) or *arc5* (right) background with low levels of the fusion protein. (C) In vivo GFP fluorescence in transgenic plants with low (left) or high (center) levels of AtFtsZ1-1–GFP, or immunofluorescence labeling of AtFtsZ1-1 in transgenic plants with high levels of AtFtsZ1-1 (right). All images are of mesophyll cells. Bright-field images are shown at bottom. The plants shown at left, center, and right are the same as those represented in lanes 3 and 4, 5 and 6, and 7 and 8 of A, respectively. (D) In vivo GFP fluorescence in pavement cells (left) or guard cells (right) of leaf epidermis in transgenic plants with high levels of AtFtsZ1-1–GFP. Arrowheads point to AtFtsZ1-1–GFP in epidermal chloroplasts; arrows (left) indicate AtFtsZ1-1–GFP in chloroplasts of underlying mesophyll cells that are also in the focal plane. Corresponding bright-field images are shown at bottom. Bars: (B) 5 μm; (C and D) 10 μm.

AtFtsZ1-1 could be detected in similar structures by immunofluorescence microscopy in *AtFtsZ1-1* overexpression lines, but not in wild-type plants (not shown).

Overall, the behavior of the AtFtsZ1-1–GFP fusion protein paralleled that of the native protein, both with respect to its localization patterns and with regard to its dosage-dependent impact on plastid division. We conclude that the AtFtsZ1-1–GFP fusion protein accurately reflects the activity of AtFtsZ1-1 in vivo.

FtsZ1 and FtsZ2 Rings Are Present in Chloroplasts of Other Plants

To determine whether FtsZ1 and FtsZ2 proteins assemble into rings in plants other than *Arabidopsis*, the anti–AtFtsZ1-1 and anti–AtFtsZ2-1 antibodies were used to detect cross-reactive proteins in pea and tobacco. On immunoblots of leaf extracts, each antibody recognized polypeptides that migrated close to those in *Arabidopsis* (Fig. 5 A). Immunofluorescence staining revealed cross-reactive proteins localized to rings at the constriction of dividing chloroplasts in both pea and tobacco (Fig. 5 B). These results suggest that FtsZ1 and FtsZ2 proteins assemble into ring structures and most likely have similar functions in plastid division in all flowering plants.

Discussion

FtsZ1 and FtsZ2 Colocalize to Rings at the Plastid Midpoint

We have shown by immunofluorescence microscopy, using antipeptide antibodies that specifically recognize either FtsZ1 or FtsZ2 in *Arabidopsis*, and by detection of an AtFtsZ1-1–GFP fusion protein in transgenic plants, that both FtsZ1 and FtsZ2 are localized to rings at the chloroplast midpoint. These results are significant in several respects. First, they constitute the first direct demonstration that chloroplast division in plants is mediated by assembly of FtsZ-containing rings at the division site. Second, they reveal that, although FtsZ1 and FtsZ2 play distinct roles in plastid division, both proteins function via ring formation.

Published April 2, 2001

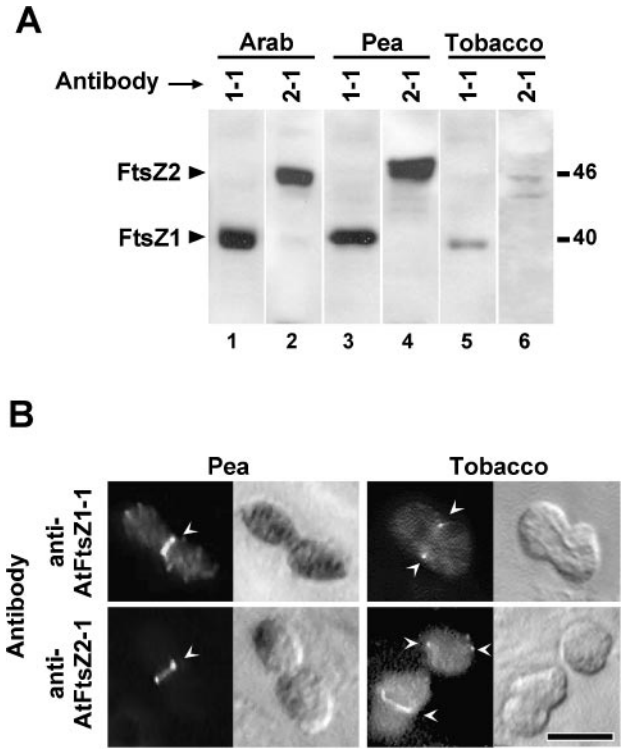

Figure 5. Detection of FtsZ1 and FtsZ2 proteins in pea and tobacco. (A) Immunoblots of leaf extracts from *Arabidopsis* (lanes 1 and 2), pea (lanes 3 and 4), or tobacco (lanes 5 and 6) were probed with affinity-purified antibodies raised against *Arabidopsis* AtFtsZ1-1 (1-1) or AtFtsZ2-1 (2-1). The identities of the immunoreactive polypeptides and migration of molecular weight markers are shown at left and right, respectively. (B) Immunofluorescence labeling (arrowheads) in pea or tobacco leaf sections probed with anti–AtFtsZ1-1 (top) or anti–AtFtsZ2-1 (bottom) antibodies. Bright-field images are also shown. Bar, 5 μm.

Third, the fact that FtsZ1 and FtsZ2 rings are associated with nonconstricted as well as constricted chloroplasts suggests that both proteins function throughout the plastid division cycle. Fourth, the detection of cross-reacting, similarly localized FtsZ rings in chloroplasts of pea and tobacco using antibodies that specifically recognize FtsZ1 or FtsZ2 proteins in *Arabidopsis* provides evidence that members of both protein families are present in all flowering plants and perform equivalent functions in plastid division. The localization of the FtsZ1 and FtsZ2 rings revealed by these studies corresponds with descriptions of the electron-dense PD rings observed in many ultrastructural investigations of chloroplast division (Kuroiwa et al., 1998) and strongly suggests that FtsZ1 and FtsZ2 are both PD ring components.

Although we have established that FtsZ1 and FtsZ2 proteins assemble into rings at the site of plastid constriction, the resolution of immunofluorescence microscopy is insufficient to allow us to determine their disposition with respect to the two envelope membranes. Based on the finding that AtFtsZ1-1 and AtFtsZ2-1 are both essential for plastid division in *Arabidopsis*, even though only AtFtsZ1-1 appears to be targeted to the chloroplast, and on ultrastructural studies describing electron-dense PD rings on the stromal and cytosolic surfaces of the envelope membranes (Kuroiwa et al., 1998), we previously proposed a working model for the arrangement of the division apparatus postulating that FtsZ1 proteins were components of the stromal PD ring, whereas FtsZ2 proteins were components of the cytosolic PD ring (Osteryoung et al., 1998). However, preliminary experiments from our laboratory suggest that AtFtsZ2-1 may not be positioned on the external surface of the chloroplast as hypothesized previously (McAndrew, R.S., and K.W. Osteryoung, unpublished observations). In a related study, Kuroiwa et al. (1999) failed to detect FtsZ in the cytosolic PD ring in red algae by immunogold labeling using antibodies generated against *Bacillus subtilis* FtsZ, although the relevance of those findings was unclear as immunological cross-reactivity against the algal FtsZ proteins was not clearly demonstrated in that report. However, two FtsZ2-like proteins from *Physcomitrella* were both shown recently to accumulate in the chloroplast stroma when expressed as GFP fusion proteins (Kiessling et al., 2000) and it remains a possibility that AtFtsZ2-1 could also be localized in the stroma, even though it was not imported in vitro (Osteryoung and McAndrew, 2001). It is also possible that AtFtsZ2-1 could be situated in the intermembrane space, consistent with the observation of a third PD ring localized in this chloroplast subcompartment in red algae (Miyagishima et al., 1998). Interestingly, proteins related to dynamins, which, like FtsZ, assemble into rings and spirals, have been shown recently to mediate division of mitochondria in yeast and animals, and are localized on the surface and in the intermembrane space of this organelle (Bleazard et al., 1999; Labrousse et al., 1999; Wong et al., 2000).

FtsZ1 and FtsZ2 Can Form Filaments Independently of One Another In Vivo

If AtFtsZ1-1 and AtFtsZ2-1 are shown to reside in the same chloroplast subcompartment, this might suggest that they assemble as heteropolymers, analogous to those formed by α- and β-tubulin. However, one set of observations is consistent with the possibility that FtsZ1 and FtsZ2 could be components of distinct structures. In transgenic *Arabidopsis* plants in which AtFtsZ1-1 was depleted to nearly undetectable levels by antisense repression, AtFtsZ2-1 still assembled into filaments which, though disordered and more numerous than in wild-type, appeared to be localized at the chloroplast periphery and exhibited a significant degree of curvature, often forming irregularly shaped rings (Fig. 2). The converse was also true, i.e., AtFtsZ1-1 filaments, often short but occasionally long and curved, were observed in the enlarged chloroplasts of plants depleted of AtFtsZ2-1 (Fig. 2), though in this case we cannot rule out that a second *Arabidopsis* FtsZ2 isoform, AtFtsZ2-2 (Osteryoung et al., 1998; Osteryoung and McAndrew, 2001), contributed to FtsZ1 assembly in these plants. Nevertheless, these observations suggest that FtsZ1 and FtsZ2 do not require one another for their assembly into cytoskeletal-like filaments competent for membrane association in vivo. However, it is not clear whether the FtsZ rings observed in wild-type chloroplasts are composed of separate FtsZ1 and FtsZ2 homopolymeric structures or whether it is a single heteropolymeric ring containing both proteins. Additional studies now underway should reveal definitively the suborganellar localization of the FtsZ1- and FtsZ2-containing rings, and, if they are localized in the same chloroplast subcompart-

Published April 2, 2001

ment, establish whether they are components of identical or distinct ring structures.

AtFtsZ1-GFP Behaves Similarly to AtFtsZ1-1 in Transgenic Plants

Immunofluorescence microscopy in fixed, embedded plant tissue provides only a static picture of FtsZ localization. To begin developing a system for studying FtsZ dynamics in living plant cells, we generated plants expressing transgenes encoding AtFtsZ1-1 or AtFtsZ2-1 fused to GFP. Similar approaches have proven invaluable for studies of FtsZ behavior in bacteria (Ma et al., 1996; Hale and de Boer, 1997; Sun and Margolin, 1998). The localization of AtFtsZ1-1–GFP depended on the degree of fusion protein accumulation, as gauged by immunoblotting and fluorescence intensity. At low levels, AtFtsZ1-1–GFP localization was restricted primarily to a ring at the chloroplast midpoint (Fig. 4, B and C, left), indicating that the GFP tag did not interfere with the ability of the fusion protein to interact with the plastid division machinery. At higher levels, the midplastid localization of AtFtsZ1-1–GFP was not obvious, but many disorganized AtFtsZ1-1–GFP filaments were observed and these were associated with severe chloroplast division defects. A similar inhibitory effect on chloroplast division was documented in transgenic *Arabidopsis* plants with AtFtsZ1-1 levels threefold or more above those in wild-type (Stokes et al., 2000) and in moss cells transfected with GFP-tagged forms of *Physcomitrella* FtsZ (Kiessling et al., 2000). These division defects may result from an imbalance in plastid division components, since in bacteria the block in cell division that accompanies FtsZ overexpression (Ward and Lutkenhaus, 1985) can be suppressed by simultaneous overexpression of other cell division proteins (Dai and Lutkenhaus, 1992; Hale and de Boer, 1997). Overall, the behavior of AtFtsZ1-1–GFP was consistent with that of the untagged protein, suggesting that the fusion protein will be valuable in future studies of FtsZ1 dynamics in vivo. However, because of the plastid division defects associated with elevated FtsZ levels, many experiments involving detection of FtsZ-GFP in living chloroplasts will have to be performed using plants that accumulate only low levels of the fusion protein.

In contrast to AtFtsZ1-1–GFP, an AtFtsZ2-1–GFP fusion protein could not be detected by fluorescence microscopy in transgenic plants (results not shown). Similarly, AtFtsZ2-1 without the GFP tag also failed to accumulate to levels significantly above those in wild-type when expressed under the control of the CaMV 35S promoter (Stokes et al., 2000). These findings could indicate that the AtFtsZ2-1 and AtFtsZ1-1 protein levels are regulated differentially. However, another possibility that has recently come to light is that the open reading frame used in construction of the *AtFtsZ2-1* and *AtFtsZ2-1*–GFP transgenes, which was based on that predicted from the *AtFtsZ2-1* genomic and cDNA sequences, may not comprise the entire AtFtsZ2-1 protein (Osteryoung and McAndrew, 2001). An in-frame Met codon 243 nucleotides (81 codons) upstream from the predicted *AtFtsZ2-1* start site could represent the true translational initiation site based on comparison to other FtsZ2 sequences, potentially explaining the failure of AtFtsZ2-1 (Stokes et al., 2000) and AtFtsZ2-1–GFP to accumulate in transgenic *Arabidopsis* and perhaps the finding that AtFtsZ2-1 was not imported into isolated chloroplasts in vitro (Osteryoung et al., 1998). We are currently investigating this possibility. Fusions of GFP to two FtsZ2-like proteins from *Physcomitrella* did accumulate to significant levels in chloroplasts in that organism (Kiessling et al., 2000).

Do FtsZ Proteins Have Other Cytoskeletal Functions in the Chloroplast?

Recently, Kiessling et al. (2000) described the presence of FtsZ-containing, cytoskeletal-like networks in the chloroplasts of *Physcomitrella*. These were visualized by transient expression of the two *Physcomitrella* chloroplast FtsZ-GFP fusion proteins referred to above. Our current and previous results regarding the effects of AtFtsZ1-1 and AtFtsZ1-1–GFP accumulation and localization in *Arabidopsis* parallel those of the moss study in two respects. First, AtFtsZ1-1, AtFtsZ1-1–GFP, and the two moss fusion proteins all behaved similarly in their transgenic hosts, causing dosage-dependent defects in plastid division. Second, all of these proteins could be detected in filamentous networks when they were overexpressed. The authors of the *Physcomitrella* study proposed that these networks represent a normally occurring in vivo structure which they termed the "plastoskeleton" and postulated its involvement in maintaining chloroplast integrity (Kiessling et al., 2000). The idea that FtsZ proteins perform multiple cytoskeletal functions in the chloroplast, as do their tubulin counterparts in the cytosol, is suggested by various other lines of evidence as well. These include numerous descriptions of chloroplast tubules in electron micrographs (McFadden, 2000), our previous finding that high levels of *AtFtsZ1-1* overexpression result in significant abnormalities in chloroplast morphology (Stokes et al., 2000), and our present finding that AtFtsZ1-1–GFP can be detected in thin connections between chloroplasts that may represent "stromules" (Kohler et al., 1997), perhaps suggesting a role for FtsZ1 in their formation or function. However, in other respects, our results are not entirely consistent with this view. We observed brightly fluorescent FtsZ-containing networks in *Arabidopsis* chloroplasts only when FtsZ levels deviated from those in wild-type. This occurred whether FtsZ levels were elevated (Fig. 4 C) or reduced (Fig. 2). Under conditions in which FtsZ levels were not significantly altered, the fluorescence signal, whether from GFP or immunofluorescence labeling, was concentrated at the plastid midpoint and the few additional filaments observed were associated with the chloroplast periphery. In contrast, the FtsZ-GFP networks observed in *Physcomitrella* were numerous, resembling those in *Arabidopsis* plants containing high levels of AtFtsZ1–1 or AtFtsZ1-1–GFP, and they traversed the chloroplast interior. The transgenes encoding the fusion proteins in the *Physcomitrella* study incorporated the CaMV 35S promoter and the plastoskeletons were visualized in the context of FtsZ overexpression. Taken together, these observations suggest that assembly of chloroplast FtsZ proteins into highly elaborated filament networks may be an artifact of perturbing the balance between different FtsZ proteins, or between FtsZs and other plastid division proteins. Alternatively, it is possible that native plastoskeletal filaments are too thin, too few in number, or too transient in nature to be readily observed by immunofluorescence microscopy in wild-type cells, or perhaps that FtsZ proteins are organized differently and perform different functions in the chloro-

Published April 2, 2001

plasts of vascular and nonvascular plants. Determining whether the plastoskeleton represents a normal or anomalous configuration of FtsZ will clearly require additional experimentation. Regardless, the ability of plant FtsZ proteins to assemble into rings and filaments in vivo undoubtedly reflects a structurally significant aspect of their biological function in the chloroplast.

We thank Travis Gallagher for maintenance of plant material and Dr. John Bowman for providing vectors.

This work was supported by National Science Foundation grant MCB-9604412.

Submitted: 26 December 2000
Revised: 5 February 2001
Accepted: 6 February 2001

References

Beech, P.L., and P.R. Gilson. 2000. FtsZ and organelle division in protists. *Protist*. 151:11–16.

Beech, P.L., T. Nheu, T. Schultz, S. Herbert, T. Lithgow, P.R. Gilson, and G.I. McFadden. 2000. Mitochondrial FtsZ in a chromophyte alga. *Science*. 287: 1276–1279.

Bi, E., and J. Lutkenhaus. 1991. FtsZ ring structure associated with division in *Escherichia coli*. *Nature*. 354:161–164.

Bleazard, W., J.M. McCaffery, E.J. King, S. Bale, A. Mozdy, Q. Tieu, J. Nunnari, and J.M. Shaw. 1999. The dynamin-related GTPase Dnm1 regulates mitochondrial fission in yeast. *Nat. Cell Biol*. 1:298–304.

Bramhill, D. 1997. Bacterial cell division. *Annu. Rev. Cell Dev. Biol*. 13:395–424.

Colletti, K.S., E.A. Tattersall, K.A. Pyke, J.E. Froelich, K.D. Stokes, and K.W. Osteryoung. 2000. A homologue of the bacterial cell division site-determining factor MinD mediates placement of the chloroplast division apparatus. *Curr. Biol*. 10:507–516.

Dai, K., and J. Lutkenhaus. 1992. The proper ratio of FtsZ to FtsA is required for cell division to occur in *Escherichia coli*. *J. Bacteriol*. 174:6145–6151.

Davis, S.J., and R.D. Vierstra. 1996. Soluble derivatives of green fluorescent protein (GFP) for use in *Arabidopsis thaliana*. *Weeds World*. 3:43–48.

de Boer, P.A.J., R.E. Crossley, and L.I. Rothfield. 1989. A division inhibitor and a topological specificity factor coded for by the minicell locus determine proper placement of the division septum in *E. coli*. *Cell*. 56:641–649.

Erickson, H.P. 2000. Dynamin and FtsZ: missing links in mitochondrial and bacterial division. *J. Cell Biol*. 148:1103–1105.

Erickson, H.P., D.W. Taylor, K.A. Taylor, and D. Bramhill. 1996. Bacterial cell division protein FtsZ assembles into protofilament sheets and minirings, structural homologs of tubulin polymers. *Proc. Natl. Acad. Sci. USA*. 93:519–523.

Gaikwad, A., V. Babbarwal, V. Pant, and S.K. Mukherjee. 2000. Pea chloroplast FtsZ can form multimers and correct the thermosensitive defect of an *Escherichia coli ftsZ* mutant. *Mol. Gen. Genet*. 263:213–221.

Gleave, A.P. 1992. A versatile binary vector system with a T-DNA organizational structure conducive to efficient integration of cloned DNA into the plant genome. *Plant Mol. Biol*. 20:1203–1207.

Gray, M.W. 1999. Evolution of organellar genomes. *Curr. Opin. Genet. Dev*. 9:678–687.

Hale, C.A., and P.A.J. de Boer. 1997. Direct binding of FtsZ to ZipA, an essential component of the septal ring structure that mediates cell division in *E. coli*. *Cell*. 88:175–185.

Kanamaru, K., M. Fujiwara, M. Kim, A. Nagashima, E. Nakazato, K. Tanaka, and H. Takahashi. 2000. Chloroplast targeting, distribution and transcriptional fluctuation of AtMinD1, a Eubacteria-type factor critical for chloroplast division. *Plant Cell Physiol*. 41:1119–1128.

Kiessling, J., S. Kruse, S.A. Rensing, K. Harter, E.L. Decker, and R. Reski. 2000. Visualization of a cytoskeleton-like FtsZ network in chloroplasts. *J. Cell Biol*. 151:945–950.

Kohler, R.H., J. Cao, W.R. Zipfel, W.W. Webb, and M.R. Hanson. 1997. Exchange of protein molecules through connections between higher plant plastids. *Science*. 276:2039–2042.

Kuroiwa, T., H. Kuroiwa, A. Sakai, H. Takahashi, K. Toda, and R. Itoh. 1998. The division apparatus of plastids and mitochondria. *Int. Rev. Cytol*. 181:1–41.

Kuroiwa, T., M. Takahara, S. Miyagishima, Y. Ohashi, F. Kawamura, and H. Kuroiwa. 1999. The FtsZ protein is not located on outer plastid dividing rings. *Cytologia*. 64:333–342.

Labrousse, A.M., M.D. Zappaterra, D.A. Rube, and A.M. van der Bliek. 1999. *C. elegans* dynamin-related protein DRP-1 controls severing of the mitochondrial outer membrane. *Mol. Cell*. 4:815–826.

Leech, R.M. 1976. The replication of plastids in higher plants. *In* Cell Division in Higher Plants. M.M. Yeoman, editor. Academic Press, London. 135–159.

Leech, R.M., and N.R. Baker. 1983. The development of photosynthetic capacity in leaves. *In* The Growth and Functioning of Leaves. J.E. Dale and F.L. Milthorpe, editors. Cambridge University Press, Cambridge. 271–307.

Löwe, J., and L.A. Amos. 1998. Crystal structure of the bacterial cell-division protein FtsZ. *Nature*. 391:203–206.

Lutkenhaus, J., and S.G. Addinall. 1997. Bacterial cell division and the Z ring. *Annu. Rev. Biochem*. 66:93–116.

Ma, X., D.W. Ehrhardt, and W. Margolin. 1996. Colocalization of cell division proteins FtsZ and FtsA to cytoskeletal structures in living *Escherichia coli* cells by using green fluorescent protein. *Proc. Natl. Acad. Sci. USA*. 93: 12998–13003.

Margolin, W. 2000. Themes and variations in prokaryotic cell division. *FEMS Microbiol. Rev*. 24:531–548.

Martin, W., B. Stoebe, V. Goremykin, S. Hansmann, M. Hasegawa, and K.V. Kowallik. 1998. Gene transfer to the nucleus and the evolution of chloroplasts. *Nature*. 393:162–165.

McFadden, G.I. 1999. Endosymbiosis and evolution of the plant cell. *Curr. Opin. Plant Biol*. 2:513–519.

McFadden, G.I. 2000. Skeletons in the closet. How do chloroplasts stay in shape? *J. Cell Biol*. 151:F19–F22.

Miyagishima, S., R. Itoh, K. Toda, H. Takahashi, H. Kuroiwa, and T. Kuroiwa. 1998. Identification of a triple ring structure involved in plastid division in the primitive red alga *Cyanidioschyzon merolae*. *J. Electron Microsc*. 47:269–272.

Negoescu, A., F. Labat-Moleur, P. Lorimier, L. Lamarcq, C. Guillermet, E. Chambaz, and E. Brambilla. 1994. F(ab) secondary antibodies: a general method for double immunolabeling with primary antisera from the same species. Efficiency control by chemiluminescence. *J. Histochem. Cytochem*. 42:433–437.

Osteryoung, K.W. 2000. Organelle fission: crossing the evolutionary divide. *Plant Physiol*. 123:1213–1216.

Osteryoung, K.W., and R.S. McAndrew. 2001. The plastid division machine. *Annu. Rev. Plant Physiol. Plant Mol. Biol*. 52:315–333.

Osteryoung, K.W., and E. Vierling. 1995. Conserved cell and organelle division. *Nature*. 376:473–474.

Osteryoung, K.W., K.D. Stokes, S.M. Rutherford, A.L. Percival, and W.Y. Lee. 1998. Chloroplast division in higher plants requires members of two functionally divergent gene families with homology to bacterial *ftsZ*. *Plant Cell*. 10:1991–2004.

Pyke, K.A., and R.M. Leech. 1992. Chloroplast division and expansion is radically altered by nuclear mutations in *Arabidopsis thaliana*. *Plant Physiol*. 99: 1005–1008.

Raskin, D.M., and P.A.J. de Boer. 1997. The MinE ring: an FtsZ-independent cell structure required for selection of the correct division site in *Escherichia coli*. *Cell*. 91:685–694.

Raskin, D.M., and P.A. de Boer. 1999a. MinDE-dependent pole-to-pole oscillation of division inhibitor MinC in *Escherichia coli*. *J. Bacteriol*. 181:6419–6424.

Raskin, D.M., and P.A. de Boer. 1999b. Rapid pole-to-pole oscillation of a protein required for directing division to the middle of *Escherichia coli*. *Proc. Natl. Acad. Sci. USA*. 96:4971–4976.

Robertson, E.J., S.M. Rutherford, and R.M. Leech. 1996. Characterization of chloroplast division using the *Arabidopsis* mutant arc5. *Plant Physiol*. 112: 149–159.

Rothfield, L., S. Justice, and J. Gracia-Lara. 1999. Bacterial cell division. *Annu. Rev. Genet*. 33:423–428.

Shi, S.-R., R.J. Cote, and C.R. Taylor. 1997. Antigen retrieval immunocytochemistry: past, present, and future. *J. Histochem. Cytochem*. 45:327–343.

Steedman, H.F. 1957. A new ribboning embedding medium for histology. *Nature*. 179:1345.

Stokes, K.D., R.S. McAndrew, R. Figueroa, S. Vitha, and K.W. Osteryoung. 2000. Chloroplast division and morphology are differentially affected by overexpression of *FtsZ1* and *FtsZ2* genes in *Arabidopsis*. *Plant Physiol*. 124: 1668–1677.

Strepp, R., S. Scholz, S. Kruse, V. Speth, and R. Reski. 1998. Plant nuclear gene knockout reveals a role in plastid division for the homolog of the bacterial cell division protein FtsZ, an ancestral tubulin. *Proc. Natl. Acad. Sci. USA*. 95:4368–4373.

Sun, Q., and W. Margolin. 1998. FtsZ dynamics during the division cycle of live *Escherichia coli* cells. *J. Bacteriol*. 180:2050–2056.

Takahara, M., H. Takahashi, S. Matsunaga, S. Miyagishima, H. Takano, A. Sakai, S. Kawano, and T. Kuroiwa. 2000. A putative mitochondrial *ftsZ* gene is present in the unicellular primitive red alga *Cyanidioschyzon merolae*. *Mol. Gen. Genet*. 264:452–460.

Vitha, S., F. Baluska, J. Jasik, D. Volkmann, and P. Barlow. 2000. Steedman's wax for F-actin visualization. *In* Actin: A Dynamic Framework for Multiple Plant Cell Function. C.J. Staiger, F. Baluska, D. Volkmann, and P. Barlow, editors. Kluwer, Dordrecht, Netherlands. 619–636.

Ward, J.E., Jr., and J. Lutkenhaus. 1985. Overproduction of FtsZ induces minicell formation in *E. coli*. *Cell*. 42:941–949.

Wong, E.D., J.A. Wagner, S.W. Gorsich, J.M. McCaffery, J.M. Shaw, and J. Nunnari. 2000. The dynamin-related GTPase, Mgm1p, is an intermembrane space protein required for maintenance of fusion competent mitochondria. *J. Cell Biol*. 151:341–352.